Jpn. J. Histor. Bot. Vol. 19 Nos. 1–2 p. 117–124 April 2011 植生史研究

Ken Watanabe[1], Hisashi Abe[1,*], Yutaka Kataoka[1] and Shuichi Noshiro[1]: Species separation of aging and degraded solid wood using near infrared spectroscopy

Abstract Applicability of near infrared (NIR) spectroscopy to identify species of degraded and aging solid wood was examined among species important to Japanese art history and archaeology. NIR spectra were obtained from wood blocks of five softwood species collected over the last 80 years from various sites and stored in the wood library of the Forestry and Forest Products Research Institute, Tsukuba in Japan. Partial least square (PLS) discriminant analysis was employed for the separation of three pairs of species, i.e., *Chamaecyparis obtusa* and *Torreya nucifera*, *Chamaecyparis obtusa* and *Chamaecyparis pisifera*, *Thuja standishii* and *Cryptomeria japonica*. The effects of spectral pre-processing and wavelength range were also evaluated. Under the limitation of sample volume, PLS discriminant analysis calibrated using second derivatives and wavelengths spanning 830 to 1150 nm could separate the samples into each pair of species in the 100 % accuracy. These results suggest that NIR spectroscopy combined with PLS discriminant analysis is a powerful technique for distinguishing species for degraded and aging wood nondestructively without any sample preparations.

Introduction

The identification of wood species is important not only for timber industry, but also for such purposes as ecology, art history, archeology, forensics, and customs procedures (e.g., Kaneko et al., 1998, 2003, 2010; Noshiro et al., 2002, 2007; Abe et al., 2005). A piece of wood is usually identified based on anatomical characteristics observed under a microscope. However, occasionally it is difficult to separate tree species or genera that have similar anatomical characteristics, especially for conifer species belonging to Cupressaceae and Taxodiaceae that have few distinct differences in anatomical characteristics (IAWA Committee, 2004).

In Japan, wood of Cupressaceae, Taxodiaceae, and Taxaceae were frequently used for Buddhist statues made during the 7–9th centuries AD (Kaneko et al., 1998, 2003, 2010). For the identification of the wood used for the construction of these statues, we collected small pieces of wood that were naturally removed from the statues. The samples were then identified by means of observation with a light microscope and/or a scanning electron microscope. In Japan it is prohibited to obtain samples directly from cultural property, and it was sometimes difficult to obtain wood samples of sufficient quality and quantity for identification. Thus, it is important to develop new alternative methods to investigate these wooden statues using nondestructive techniques.

The chemical composition, especially second metabolites of wood, have been used for taxonomic purposes (Erdtman, 1963), and the identification and classification of wood species were tried on some species of conifers of Pinaceae and Cupressaceae (Erdtman, 1963; Zavarin et al., 1967). Recently, spectroscopic methods, such as infrared, ultraviolet, and nuclear magnetic resonance, were employed for the identification of wood species based on their chemical composition (Nuoppenen et al., 2006; Huang et al., 2008). Among the aforementioned spectroscopic methods, near infrared (NIR) spectroscopy is not affected by atmospheric conditions compared to the other methods, and this technology has become popular because of its utility and availability.

The application of NIR spectroscopy for the identification and classification of wood species has been improving since the publication of seminal papers by Schimleck et al. (1996) and Brunner et al. (1996). Both used principal components analysis (PCA) and the subsequent score plots to show the potential of NIR spectroscopy to differentiate between wood samples of various species. Since then, the successful identification of wood species or wood-based materials has been carried out using NIR spectroscopy combined with several chemometric analyses, such as the Mahalanobis' generalized distance (Tsuchikawa et al., 2003a, 2003b; Tsuchikawa & Yamato, 2003), K nearest neighbors

[1] Forestry and Forest Products Research Institute, 1 Matsunosato, Tsukuba, Ibaraki 305-8687, Japan
* Corresponding author (e-mail: abeq@affrc.go.jp)

(Tsuchikawa et al., 2003b; Tsuchikawa & Yamato, 2003), soft independent modeling of class analogy (SIMCA) (Tsuchikawa et al., 2003b; Tsuchikawa & Yamato, 2003; Gierlinger et al., 2004; Adedipe et al., 2008), and partial least square (PLS) discriminant analysis (Furumoto et al., 1999; Flæte et al., 2006).

These studies were, however, restricted to small clean samples with ideal highly controlled conditions because the NIR spectra are influenced by surface roughness (Hein et al., 2010) as well as the physical and chemical properties of the wood. In these papers, the NIR spectra were obtained from samples collected from a single site, or the irradiation surfaces were carefully cut in the same manner. Because wood has inherent anatomical and morphological variability within species, it is still unknown whether NIR spectroscopy is applicable for the species identification of aging and/or degraded wood that has been collected from various sites. Such conditions are common in the study of ancient wooden statues. To evaluate the applicability of NIR spectroscopy to identify the species of degraded and aging wood, three pairs of five historically important conifer species used in the construction of wooden statues in Japan was studied using NIR spectroscopy.

Materials and Methods

1. Sample preparation

Wood specimens of five species that were collected from various sites in Japan and stored over the past 80 years in the wood library of the Forestry and Forest Products Research Institute, Tsukuba (TWTw) in Japan were used in our analysis (Table 1). They include 18 specimens of *Chamaecyparis obtusa*, 19 of *Torreya nucifera*, 11 of *Thuja standishii*, 19 of *Chamaecyparis pisifera,* and 24 of *Cryptomeria japonica*. The specimens were stored in the collection room, which is

Table 1 Samples used in this study showing the years and sites of collection

Sample no.	Species	TWTw no.	Calibration/ Validation set	Collection years	Collection sites
1	*Chamaecyparis obtusa*	1168	calibration	1928	Saitama
2	*Chamaecyparis obtusa*	11951	calibration		Saitama
3	*Chamaecyparis obtusa*	12166	calibration	1931	Yaku Isl.
4	*Chamaecyparis obtusa*	13263	calibration	1970	Chiba
5	*Chamaecyparis obtusa*	1345	calibration		Saitama
6	*Chamaecyparis obtusa*	14666	calibration		Tokyo
7	*Chamaecyparis obtusa*	15	calibration		Tokyo
8	*Chamaecyparis obtusa*	1770	calibration		Tochigi
9	*Chamaecyparis obtusa*	2264	calibration		unknown
10	*Chamaecyparis obtusa*	4791	calibration		unknown
11	*Chamaecyparis obtusa*	7991	calibration		Nagano
12	*Chamaecyparis obtusa*	873	calibration		Nagano
13	*Chamaecyparis obtusa*	14665	validation		Chiba
14	*Chamaecyparis obtusa*	14668	validation		unknown
15	*Chamaecyparis obtusa*	18791	validation	2000	Miyazaki
16	*Chamaecyparis obtusa*	3329	validation	1929	Chiba
17	*Chamaecyparis obtusa*	6371	validation	1981	Tokyo
18	*Chamaecyparis obtusa*	9293	validation	1961	Nagano
19	*Torreya nucifera*	12158	calibration	1931	Kumamoto
20	*Torreya nucifera*	14506	calibration	1964	Tokyo
21	*Torreya nucifera*	14507	calibration		Tokyo
22	*Torreya nucifera*	14755	calibration		Chiba
23	*Torreya* sp.*	15979	calibration		China
24	*Torreya nucifera*	18403	calibration	2000	Okayama
25	*Torreya nucifera*	19683	calibration	2002	Tsushima Isl.
26	*Torreya* sp.**	20112	calibration		unknown
27	*Torreya nucifera*	3321	calibration	1929	Chiba
28	*Torreya nucifera*	4332	calibration	1981	Saitama
29	*Torreya nucifera*	471	calibration	1950	Chiba
30	*Torreya nucifera*	4772	calibration		unknown
31	*Torreya nucifera*	1191	validation	1928	Saitama
32	*Torreya nucifera*	11938	validation		Saitama
33	*Torreya nucifera*	13247	validation	1970	Chiba
34	*Torreya nucifera*	13662	validation	1987	Tokyo
35	*Torreya nucifera*	14504	validation		Tokyo
36	*Torreya* sp.*	15978	validation		China
37	*Torreya nucifera*	852	validation		Miyazaki
38	*Thuja standishii*	12441	calibration		unknown
39	*Thuja standishii*	14537	calibration		Chiba
40	*Thuja standishii*	24337	calibration	2008	Nagano
41	*Thuja standishii*	4790	calibration		unknown
42	*Thuja standishii*	595	calibration	1950	Saitama
43	*Thuja standishii*	875	calibration		Nagano
44	*Thuja standishii*	9295	calibration	1961	Nagano
45	*Thuja standishii*	12186	validation	1924	unknown
46	*Thuja standishii*	14639	validation		Tokyo
47	*Thuja standishii*	22003	validation	2005	Gifu
48	*Thuja standishii*	649	validation	1951	Nagano
49	*Chamaecyparis pisifera*	11952	calibration		Saitama
50	*Chamaecyparis pisifera*	13264	calibration	1970	Chiba
51	*Chamaecyparis pisifera*	1347	calibration		Saitama
52	*Chamaecyparis pisifera*	14390	calibration	1979	Tokyo
53	*Chamaecyparis pisifera*	14563	calibration		Chiba
54	*Chamaecyparis pisifera*	22065	calibration	2005	Ibaraki
55	*Chamaecyparis pisifera*	24266	calibration	2008	Nagano
56	*Chamaecyparis pisifera*	24588	calibration	2008	Miyagi
57	*Chamaecyparis pisifera*	3330	calibration	1929	Chiba
58	*Chamaecyparis pisifera*	4792	calibration		unknown
59	*Chamaecyparis pisifera*	874	calibration		Nagano
60	*Chamaecyparis pisifera*	8881	calibration		The Netherlands
61	*Chamaecyparis pisifera*	21822	calibration	2004	Hokkaido
62	*Chamaecyparis pisifera*	12169	validation		unknown
63	*Chamaecyparis pisifera*	14391	validation	1979	Tokyo
64	*Chamaecyparis pisifera*	24196	validation	2008	Nagano
65	*Chamaecyparis pisifera*	24293	validation	2008	Nagano
66	*Chamaecyparis pisifera*	651	validation	1951	Nagano
67	*Chamaecyparis pisifera*	9294	validation	1961	Nagano
68	*Cryptomeria japonica*	1173	calibration	1928	Saitama
69	*Cryptomeria japonica*	1346	calibration		Saitama
70	*Cryptomeria japonica*	14590	calibration		Chiba
71	*Cryptomeria japonica*	14593	calibration		Yaku Isl.
72	*Cryptomeria japonica*	14594	calibration		Yaku Isl.
73	*Cryptomeria japonica*	14914	calibration	1991	Ishikawa
74	*Cryptomeria japonica*	1769	calibration		Tochigi
75	*Cryptomeria japonica*	19512	calibration	2002	Amami Isl.
76	*Cryptomeria japonica*	4785	calibration		unknown
77	*Cryptomeria japonica*	6427	calibration	1983	Saitama
78	*Cryptomeria japonica*	6428	calibration	1983	Saitama
79	*Cryptomeria japonica*	6429	calibration	1983	Saitama
80	*Cryptomeria japonica*	817	calibration		Akita
81	*Cryptomeria japonica*	9290	calibration	1967	Akita
82	*Cryptomeria japonica*	9291	calibration	1967	Shizuoka
83	*Cryptomeria japonica*	96	calibration	1996	Tokyo
84	*Cryptomeria japonica*	10275	validation		unknown
85	*Cryptomeria japonica*	14591	validation		Chiba
86	*Cryptomeria japonica*	14592	validation		unknown
87	*Cryptomeria japonica*	18328	validation	1988	Akita
88	*Cryptomeria japonica*	3322	validation	1929	Chiba
89	*Cryptomeria japonica*	4787	validation		Tochigi
90	*Cryptomeria japonica*	9289	validation	1962	Miyazaki
91	*Cryptomeria japonica*	9292	validation		Aomori

*Species other than Japanese *Torreya nucifera,* **Species not identified.

conditioned with a temperature range of 20–30°C and a relative humidity of about 50–80%. The dimensions of the samples were 10 × 2 cm^2 in cross section and 15 cm long. Prior to making the NIR measurement, one of the end-grain surfaces was cut using a circular saw to expose a fresh surface, while the other end-grain surface was left untouched. Among samples of each species, two thirds were used as the calibration set, and the remaining one third were used as the validation set.

2. NIR measurement

The diffuse reflectance spectra on a spot diameter of ca. 3 mm were collected at 4 cm^{-1} intervals over the range 12,000–4000 cm^{-1} (830–2500 nm) using a MATRIX-F spectrometer (Bruker Optics) equipped with an NIR fiber optic probe in August 2010. A piece of commercial resin spectralon was used as the reference material. Five spectra were randomly collected from the heartwood zone of both end-grain surfaces (fresh and degraded surfaces), respectively. A total of 10 (5 × 2) spectra were obtained from each sample.

3. Pre-processing of NIR spectra

NIR spectra were pre-processed with multiplicative scatter correction (MSC) and Savitzky-Golay second derivations with 29 convolution points, respectively. The effect of the reduced spectral range was also evaluated. Two reduced wavelength ranges, 830–1150 and 1300–2500 nm, were selected for discriminant analysis. Previously, the visible range plus only a narrow NIR range was shown to be useful for the prediction of the chemical components in the wood (Kelley et al., 2004a) and the discrimination of wood-based materials (Tsuchikawa et al., 2003b). In contrast, wavelengths above 1300 nm were known to be associated with many absorption bands of hydroxyl groups derived from water (Bokobza, 2002) and cellulose (Mitsui et al., 2008).

4. Discriminant analysis

Partial least squares (PLS) discriminant analysis was performed using the Unscrambler software version 9.1 (CAMO, OR, USA). PLS discriminant analysis involves developing a partial least square (PLS) regression model. The PLS regression models for each pair of species, namely *Chamaecyparis obtusa* vs *Torreya nucifera*, *Chamaecyparis obtusa* vs *Chamaecyparis pisifera*, and *Thuja standishii* vs *Cryptomeria japonica*, were constructed individually using the calibration set with full cross-validation. The response variable was a binary class indicator variable instead of a continuous variable. The γ variables for one class ("species A") and the other class ("species B") were labeled with +1 and 0,

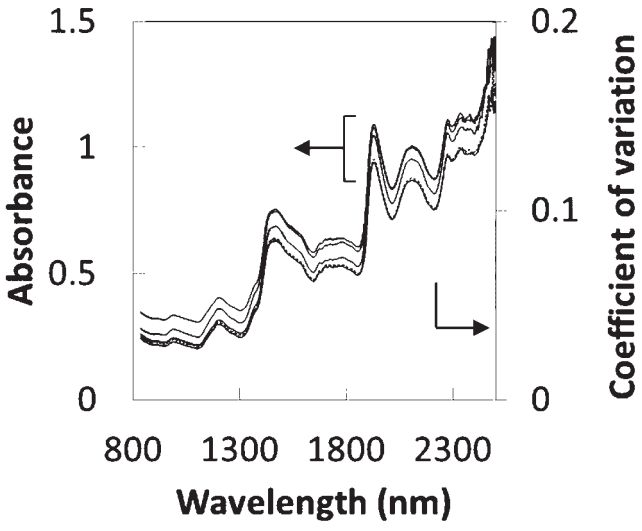

Fig. 1 Five raw spectra measured from the fresh surface of *Chamaecyparis pisifera* (TWTw-24588) and the coefficient of variation for each wavelength.

respectively. The model was then used to separate two species in the validation set by means of PLS discriminant analysis. The correct identification of "species A" was arbitrarily assigned to samples with a predicted $\gamma > 0.5$, and the correct identification of "species B"was assigned when $\gamma < 0.5$. The maximum principal components (PCs) used to compute the PLS regression models were set at four to prevent over-fitting. The optimal PCs used in the models were determined by observing the response of the residual variance with added PCs. When additional PCs did not substantially decrease the residual variance, iterations were terminated.

The fresh and degraded surfaces of each sample were individually judged as being correctly identified, when more than three out of five spectra fell into the right species. The percentage of correct identification was defined as the proportion of the number of each species identified correctly compared to the total number of each species.

Results

1. Spectroscopic characterization

The variability of the NIR spectra by the location of the NIR scan was observed in five raw spectra measured from the fresh surface of *Chamaecyparis pisifera* (TWTw-24588)(Fig. 1). The spectra shifted vertically in the overall NIR region, and it is difficult to characterize differences among the five spectra. So the coefficient of variation (CV) for each wavelength was calculated to evaluate the relationship between the wavelength

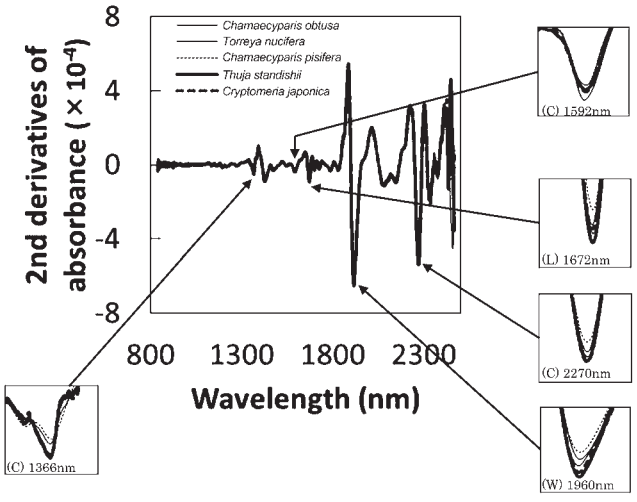

Fig. 2 The typical second derivatives of NIR spectra for each species. Absorption peaks and bands assigned to cellulose (C), lignin (L), and water (W) are shown by arrows.

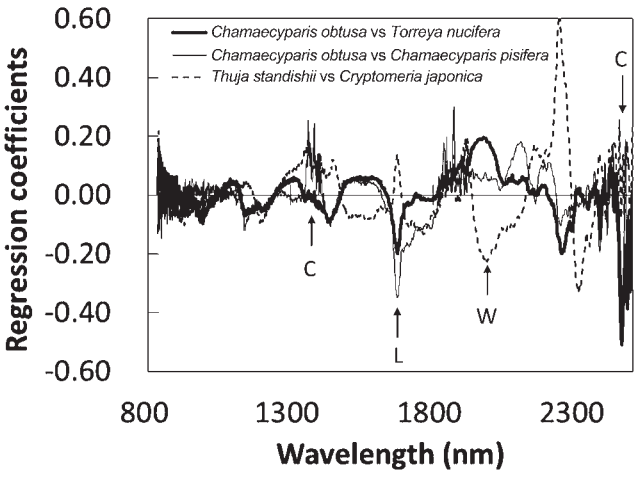

Fig. 3 Regression coefficients from the PLS regression of second derivative spectra for the separation *Chamaecyparis obtusa* vs *Torreya nucifera*, *Chamaecyparis obtusa* vs *Chamaecyparis pisifera*, and *Thuja standishii* vs *Cryptomeria japonica*, respectively. Bands assigned to cellulose (C), lignin (L), and water (W) are shown by arrows.

and the differences among the five spectra. The CV was inversely proportional to absorbance and had a tendency to decrease with increasing wavelength. The wavelength below 1300 nm showed a large CV, and a sharp decline in the CV was found at a wavelength of about 1300 nm.

Spectral difference in typical second derivative spectra from the fresh surfaces among the five species was evident at the absorption bands of 1366, 1592, 1672, 1910, and 2270 nm (Fig. 2). These absorption bands are assigned to wood components of water, cellulose, and lignin (Ali et al., 2001; Tsuchikawa & Siesler, 2003; Bokobza, 2002, Schenk et al., 2008). The absorption bands at 1366, 1592, and 2270 nm were assigned to cellulose, 1672 nm to lignin, and 1910 nm to water, respectively.

2. PLS discriminant analysis

The regression coefficients of the PLS regression models calibrated using second derivative spectra were useful to determine important spectral regions that correlate to species separation (Fig. 3). Overall, the wavelengths with an impact on the model were above 1300 nm in all pairs of species. The wavelengths with high impact were labeled in response to the absorption bands assigned to water, cellulose, and lignin (Fig. 3) (Ali et al., 2001; Tsuchikawa & Siesler, 2003; Bokobza, 2002; Schenk et al., 2008). The regression coefficients provided a strong relationship with the chemical composition of the wood. To our knowledge, no assignment to specific wood components corresponding to the absorption bands at 1870, 2245, and 2300 nm has been reported in the past studies.

The score plots of the first and second PCs for the PLS regression models showed clear separation between *Chamaecyparis obtusa* vs *Torreya nucifera*, *Chamaecyparis obtusa* vs *Chamaecyparis pisifera*, and *Thuja standishii* vs *Cryptomeria japonica* (Fig. 4). The models were developed using second derivative spectra with the wavelengths spanning 830–1150 nm. The PLS regression models showed distinct clusters in all the pairs of species, although the score plots of the degraded surfaces were widely spread compared with those of the fresh surfaces. The difference between *Thuja standishii* and *Cryptomeria japonica* was less pronounced compared to *Chamaecyparis obtusa* and *Torreya nucifera* or *Chamaecyparis obtusa* and *Chamaecyparis pisifera*. Some plots of *Cryptomeria japonica* samples overlapped with the cluster of *Thuja standishii*. Thus, another PLS regression model of *Thuja standishii* vs *Cryptomeria japonica* was constructed excluding the 21 overlapped spectra of *Cryptomeria japonica* samples that we regarded as outliers. Contrary to our expectation, the cluster difference between each species was not observed in the score plots of the PLS regression models calibrated by MSC and other wavelengths spanning 1300–2500 and 830–2500 nm (not presented here).

PLS discriminant analysis was employed to identify the validation set of six specimens of *Chamaecyp-*

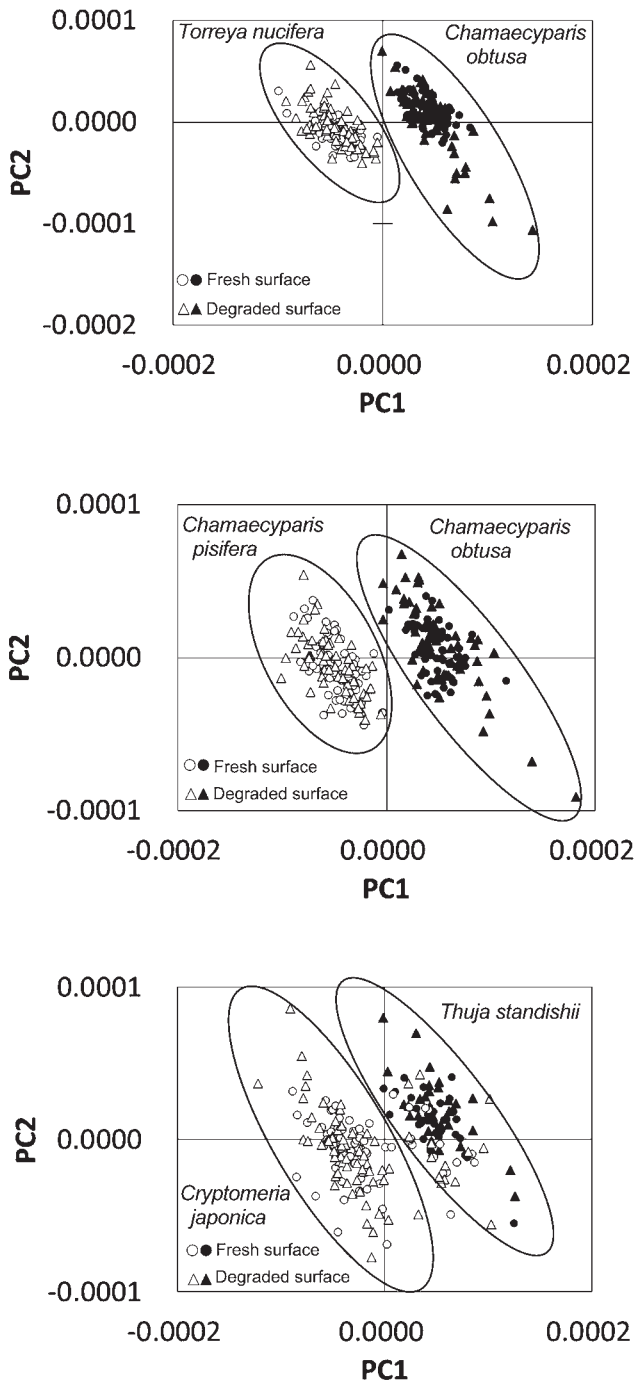

Fig. 4 PLS discriminant analysis score plots of the first and second principal components calibrated by the wavelengths spanning 830–1150 nm for (a) *Chamaecyparis obtusa* (black) vs *Torreya nucifera* (white), (b) *Chamaecyparis obtusa* (black) vs *Chamaecyparis pisifera* (white), and (c) *Thuja standishii* (black) vs *Cryptomeria japonica* (white).

aris obtusa, seven of *Torreya nucifera*, four of *Thuja standishii*, six of *Chamaecyparis pisifera* and eight of *Cryptomeria japonica*. The identification results show that the PLS regression models can provide highly separated pairs that led to their correct taxonomic identification (Table 2).

Root mean square error of prediction (RMSEP) provides an objective means of evaluating the effect of the data pre-treatment of the identification process. The ability for identification is largely reflected by the RMSEP values, with the best overall identification, being achieved in 100% accuracy using the second derivative spectra with the wavelengths spanning 830–1150 nm for each pair of species (Table 2).

Discussion

1. Spectroscopic characterization

Because of the variability of the NIR spectra within a sample (Fig. 1), we identified species for each spectrum individually without averaging the five spectra. The variability of the spectra may be explained by the size of the spot area of NIR probe and the density variation induced by annual rings. The distance between adjacent annual rings was larger than the spot diameter of 3 mm in some samples, especially those of *Chamaecyparis pisifera* and *Cryptomeria japonica*. Thus, the mean density of the spot area was different between each location of the NIR scan, resulting in the variability of the NIR spectra. The larger the spot area of the NIR probe, the less variable the results among the NIR spectra. In reality, however, the spot area is restricted by the sample size and the condition of the sample.

The CV provides the difference among the five spectra, that correspond to wavelength. The decrease of CV inversely to absorbance (Fig. 1) may be due to an increase in water absorption as wavelength increases. This inverse relationship shows that the larger the water absorption, the less variable the NIR spectra. The wavelength spanning 830–1300 nm showed a large CV, indicating that this wavelength range is more sensitive to the location of the NIR scan compared to wavelengths above 1300 nm.

Spectral differences among the five species were observed at absorption bands of 1366, 1592, 1672, 1910, and 2270 nm. The wavelengths correspond to the water, cellulose, and lignin components of the wood. This result shows that the amount of the wood components, characteristics of each species, is different among the five species.

2. PLS discriminant analysis

In the regression coefficients of the PLS regression

Table 2 Summary of validation of PLS regression models and percentages of correct identification

Separation species A vs B	Pre-processing	Wavelength (nm)	Optimal PCs	RMSEP	correct identification (%)	
					True species A	True species B
Chamaecyparis obtusa vs *Torreya nucifera*	MSC	830-2500	5	0.24	100	100
	MSC	830-1150	5	0.18	100	100
	MSC	1300-2500	4	0.26	92	100
	2nd	830-2500	5	0.23	100	100
	2nd	830-1150	4	0.13	100	100
	2nd	1300-2500	5	0.25	100	100
Chamaecyparis obtusa vs *Chamaecyparis pisifera*	MSC	830-2500	5	0.41	83	100
	MSC	830-1150	5	0.24	83	100
	MSC	1300-2500	5	0.39	75	100
	2nd	830-2500	5	0.23	100	100
	2nd	830-1150	3	0.14	100	100
	2nd	1300-2500	5	0.26	100	100
Thuja standishii vs *Cryptomeria japonica*	MSC	830-2500	5	0.33	88	100
	MSC	830-1150	5	0.24	88	100
	MSC	1300-2500	4	0.35	100	100
	2nd	830-2500	5	0.30	88	100
	2nd	830-1150	3	0.27	88	100
	2nd	1300-2500	5	0.31	88	100
	2nd*	830-1150	3	0.19	100	100

Identification for each true species. 2nd, second derivative; *, without outliers.

models, the wavelengths above 1300 nm showed a high impact on the models in all pairs of species. Thus, the wavelengths above 1300 nm, which contains the most distinct spectral information on the first overtone and combination bands (Bokobza, 2002), was expected to contribute to the separation of the species. This agrees with the suggestion by Gierlinger et al. (2004) that the NIR spectral region below 1300 nm is characterized by low intensity and a low signal-to noise ratio, and that this region was consequently not suitable for species identification. The regression coefficients provided a strong relationship with the absorption bands assigned to chemical composition, namely, water, cellulose and aromatic groups of lignin (Fig. 3), demonstrating important differences in wood chemistry between the three pairs of species. On the other hand, no assignment to specific wood components that correspond to the band peaks (1870, 2245, and 2300 nm) has been reported in the past studies. It may be possible to ascribe these unknown band peaks to anatomical wood structure, as well as other chemical components in the wood. Further studies on the assignment of the NIR absorption bands for wood components and structure are thus required.

The distinct clusters in the score plots calibrated by the wavelengths spanning 830–1150 nm (Fig. 4) demonstrate that the NIR spectra obtained from both fresh and degraded surfaces contain information that is relevant for differentiating species. On the other hand, the lack of differentiation between each species in the score plots with wavelengths spanning 1300–2500 and 830–2500 nm indicates that these wavelengths have poor identification capability compared to those spanning the 830–1150 nm range.

It is not surprising that the model using the wavelengths of 830–1150 nm showed a higher percentage of correct species identification compared to that of 1300–2500 nm (Table 2). Contrary to our expectations, however, the score plots demonstrate that the effective wavelengths for wood identification does not necessarily match the wavelength corresponding to strong regression coefficients in the PLS regression models (Fig. 3). The wavelengths spanning the 830–1150 nm range are difficult to assign to specific wood components, but can be attributed to second overtones of hydroxyls and third overtones of C-H stretching vibrations (Kelley et al., 2004b). The successful prediction of wood chemical composition using the reduced NIR spectral region was reported by Kelley et al. (2004b) and Axrup et al. (2000). Our results support the usefulness of the reduced spectral region for wood species identification, in addition to chemical composition. This reduced spectral region enables the use of a light-weight, inexpensive handheld spectrometer with rapid acquisition times. It has a huge advantage to identify wood species under field conditions.

In all pairs of species, the PLS regression models calibrated using the second derivative spectra and wavelengths spanning 830–1150 nm separated two species with 100% accuracy. The percentage of correct identification in this study were comparable to the separation of three larch species (*Larix decidua, L kaempferi,* and *L. eurolepis*) (Gierlinger et al., 2004) and three spruce species (*Picea abies*, *P. lutzii,* and *P. sitchensis*) (Flæte et al., 2006). Meanwhile, the percentage of correct identification in the SIMCA analysis for the separation of two oak species (*Quercus rubra* and *Q. alba*) (Adedipe et al., 2008) showed slightly lower percentages ranging from 80–98%.

In addition to reveal the separation of historically important softwood species, this study showed for the first time that NIR spectroscopy has a potential to identify the species of degraded and aging wood. Ali et al. (2001) showed that NIR could be used to monitor the aging of paper treated by high temperature, and that the development of carbonyl/carboxyl peak, which can be seen in the wavelength range spanning 1700–1900 nm, a characteristic of aging. It is likely that the wavelength range impacted by aging should be excluded from the identification of variably-aged wood species. Under the limitation of sample volume, it can be concluded that the PLS discriminant analysis using second derivative spectra and wavelengths spanning 830–1150 nm has the potential to separate degraded and aging wood between *Chamaecyparis obtusa* and *Torreya nucifera*, *Chamaecyparis obtusa* and *Chamaecyparis pisifera*, and *Thuja standishii* and *Cryptomeria japonica*.

Conclusions

The applicability of NIR spectroscopy to separate species of degraded and aging wood, an important application for the study of Japanese art history, was examined. NIR spectra were obtained from wood blocks of several softwood species that were collected over the past 80 years from various sites in Japan and stored in the wood library of the Forestry and Forest Products Research Institute in Japan. Partial least square (PLS) discriminant analysis was employed to discriminate between *Chamaecyparis obtusa* and *Torreya nucifera*, *Chamaecyparis obtusa* and *Chamaecyparis pisifera,* and *Thuja standishii* and *Cryptomeria japonica*. PLS discriminant analysis using second derivative and wavelengths spanning 830 to 1150 nm separated the samples into each pair of species with 100% accuracy. The results suggest that NIR spectroscopy combined with PLS discriminant analysis is a powerful tool for the identification and classification of species for degraded and aging wood using nondestructive techniques.

Acknowledgements

This research was supported by a Grant-in-Aid for Scientific Research (No21300332) from the Japan Society for the Promotion of Science (JSPS). We are grateful to Dr. Ben A. LePage for the linguistic check of the final manuscript.

References

Abe, H., Itoh, S., Shibata, M., Ogata, K., Kitin, P. & Fujii, T. 2005. Tree species of timber imported to Japan from Southeast Asia. JIRCAS Working Report No. 39: 251–253.

Adedipe, O. E., Dawson-Andoh, B., Slahor, J. & Osborn, L. 2008. Classification of red oak (*Quercus rubra*) and white oak (*Quercus alba*) wood using a near infrared spectrometer and soft independent modeling of class analogies. *Journal of Near Infrared Spectroscopy* **16**: 49–57.

Ali, M., Emsley, A. M., Herman, H. & Heywood, R. J. 2001. Spectroscopic studies of the ageing of cellulosic paper. *Polymer* **42**: 2893–2900.

Axrup, L., Markides, K. & Nilsson, T. 2000. Using miniature diode array NIR spectrometers for analyzing wood chips and bark samples in motion. *Journal of Chemometrics* **14**: 561–572.

Bokobza, L. 2002. Origin of near-infrared absorption bands. *In*: Siesler, H. W., Ozaki, Y., Kawata, S. & Heise, H. M., eds., *Near-Infrared Spectroscopy—Principles, Instruments, Applications*, 34–35. Wiley-VCH, Weinheim, Germany.

Brunner, M., Eugster, R., Trenka, E. & Bergamin-Strotz, L. 1996. FT-NIR spectroscopy and wood identification. *Holzforschung* **50**: 130–134.

Erdtman, H. 1963. Some aspects of chemotaxonomy. *In*: Swain, T. ed., *Chemical Plant Taxonomy,* 89–125. Academic Press, London, New York.

Flæte, P. O., Haartveit, E. Y . & Vadla, K. 2006. Near infrared spectroscopy with multivariate statistical modeling as a tool for differentiation of wood from tree species with similar appearance. *New Zealand Journal of Forestry Science* **36**: 382–392.

Furumoto, H., Lampe, U., Meixner, H. & Roth, C. 1999. Infrarotanalyse zur messing der holzqualität. *Holz als Roh- und Werkstoff* **57**: 23–28 (in German).

Gierlinger, N., Schwanninger, M. & Wimmer, R. 2004. Characteristics and classification of fourier-transform near infrared spectra of the heartwood of different larch species (*Larix* sp.). *Journal of Near Infrared Spectroscopy* **12**: 113–119.

Hein, P. R. G., Lima, J. T. & Chaix, G. 2010. Effects of sample preparation on NIR spectroscopic estimation of chemical properties of *Eucalyptus urophylla* S. T. Blake wood. *Holzforschung* **64**: 45–54.

Huang, A., Zhou, Q., Liu, J., Fei, B. & Sun, S. 2008. Distinc-

tion of three wood species by Fourier transform infrared spectroscopy and two-dimensional correlation IR spectroscopy. *Journal of Molecular Structure* **883–884**: 160–166.

IAWA Committee. 2004. IAWA list of microscopic features for softwood identification. *IAWA Journal* **25**: 1–70.

Kaneko, H., Iwasa, M., Noshiro, S. & Fujii, T. 1998. Wood types and material selection for Japanese wood statues of ancient period: Particularly the 7th–8th centuries. *Museum* No. 555: 3–54 (in Japanese).

Kaneko, H., Iwasa, M., Noshiro, S. & Fujii, T. 2003. Wood types and material selection for Japanese wood statues of ancient period 2: Particularly of the 8th–9th centuries. *Museum* No. 583: 5–44 (in Japanese).

Kaneko, H., Iwasa, M., Noshiro, S. & Fujii, T. 2010. Wood types and material selection for Japanese wood statues of ancient period 3: Further thoughts on 8th and 9th century sculptures. *Museum* No. 625: 61–78 (in Japanese).

Kelley, S. S., Rials, T. G., Groom, L. H. & So, C.-L. 2004a. Use of near infrared spectroscopy to predict the mechanical properties of six softwoods. *Holzforschung* **58**: 252–260.

Kelley, S. S., Rials, T. G., Snell, R., Groom, L. H. & Sluiter, A. 2004b. Use of near infrared spectroscopy to measure the chemical and mechanical properties of solid wood. *Wood Science and Technology* **38**: 257–276.

Mitsui, K., Inagaki, T. & Tsuchikawa, S. 2008. Monitoring of hydroxyl groups in wood during heat treatment using NIR spectroscopy. *Biomacromolecules* **9**: 286–288.

Noshiro, S., Suzuki, M. & Tsuji, S. 2002. Three buried forests of the Last Glacial Stage and middle Holocene at Ooyazawa on northern Honshu Island of Japan. Review of Palaeobotany and Palynology **122**: 155–169.

Noshiro, S., Suzuki, M. & Sasaki, Y. 2007. Importance of *Rhus verniciflua* Stokes (lacquer tree) in prehistoric periods in Japan, deduced from identification of its fossil woods. *Vegetation History and Archaeobotany* **16**: 405–411.

Nuoppenen, M. H., Wikberg, H. I., Birch, M. G., Jääskeläinen, A.-S., Marunu, S., Vuorinen, T. & Stewart, D. 2006. Characterization of 25 tropical hardwoods with Fourier transform infrared, ultraviolet resonance Raman, and ^{13}C-NMR cross-polarization/magic-angle spinning spectroscopy. *Journal of Applied Polymer Science* **102**: 810–819.

Schimleck, L., Michell, A. J. & Vinden, P. 1996. Eucalypt wood classification by NIR spectroscopy and principal components analysis. *Appita Journal* **49**: 319–324.

Shenk, J. S., Workman, J. J. & Westhaus, M. O. 2008. Application of NIR spectroscopy to agricultural products. *In*: Burns, D. A. & Ciurczak, E. W., eds., *Handbook of Near-Infrared Analysis*, 3rd ed., 356–357. Taylor & Francis Group, New York.

Tsuchikawa, S. & Siesler, H. W. 2003. Near-infrared spectroscopic monitoring of the diffusion process of deuterium-labeled molecules in wood. Part I: Softwood. *Applied Spectroscopy* **57**: 667–674.

Tsuchikawa, S. & Yamato, K. 2003. Discriminant analysis of wood-based materials with weathering damage by near infrared spectroscopy. *Journal of Near Infrared Spectroscopy* **11**: 391–399.

Tsuchikawa, S., Inoue, K., Noma, J. & Hayashi, K. 2003a. Application of near-infrared spectroscopy to wood discrimination. *Journal of Wood Science* **49**: 29–35.

Tsuchikawa, S., Yamato, K. & Inoue, K. 2003b. Discriminant analysis of wood-based materials using near-infrared spectroscopy. *Journal of Wood Science* **49**: 275–280.

Zavarin, E., Smith, L. & Bicho, J.G. 1967. Tropolone of Cupressaceae 3. *Phytochemistry* **6**: 1387–1394.

(Accepted: 4 Feb. 2011)